

DEVELOPMENT OF ULTRAFAST LASER-BASED MICRO-CT SYSTEM FOR SMALL ANIMAL IMAGING

A. Krol¹, J.-C. Kieffer², R. Toth², E.D. Lipson^{3,1}, R. E. Kincaid³,
I. L. Coman^{4,1}

¹SUNY Upstate Medical University, Department of Radiology, Syracuse, NY, USA

²Advanced, Laser Light Source, INRS-EMT, Québec University, Varennes, Québec, Canada

³Department of Physics, Syracuse University, Syracuse, NY, USA

⁴Department of Mathematics and Computer Science, Ithaca College, Ithaca, NY, USA

E-mail: krola@upstate.edu

ABSTRACT

We investigated performance of ultrafast (30 fs –200 fs) laser-based x-ray source as an alternative to a microfocal x-ray tube used in micro-CT systems. A number of solid targets including Ge, Mo, Rh, Ag, Sn, Ba, La Nd with matching filters was used. We optimized conditions for x-rays generation, measured x-ray spectra and obtained images of small animals using various characteristic x-ray lines and various imaging geometries. X-ray spectra produced by ultrafast laser are advantageous for micro-CT imaging because most of the emission is in narrow characteristic lines. The spectra can be rapidly changed, via target change, and easily matched to the imaging task. X-ray fluence can exceed fluence produced by conventional microfocal tube. Effective x-ray focal spot size is about 5 μm . Good quality projection images of small animals were obtained: (a) in a single energy absorption mode with single x-ray line matching animal thickness and density, and (b) in the dual-energy absorption mode with two x-ray lines bracketing absorption energy of the I-based and Ba-based contrast agent, respectively, and (c) in the *in line* phase-contrast enhancing geometry using single x-ray line matching animal thickness and density. We conclude that the ultrafast laser-based, compact, x-ray source is a promising alternative to a microfocal x-ray tube in micro-CT systems. Its utilization might result in faster scans with lower radiation dose, and with better spatial and contrast resolution. In addition, it might allow practical implementation of dual-energy and phase-contrast imaging micro-CT that not possible with conventional micro-CT.

INTRODUCTION

Recent discoveries in genomics and molecular and cell biology have led to the development and wide use of small animal models of human disease. As a result, high-resolution tomography has become an important tool in the modern biomedical research. Functional imaging of small animal models has been accomplished by introduction of micro-PET [1]-[3], and micro-SPECT [4]-[5], while anatomic imaging of soft tissue has been realized by means of magnetic resonance microscopy [6], micro-ultrasound [7] and micro-CT (especially when using a contrast medium) [8]-[10]. Micro-CT has been extensively used for bone imaging [11]. Recently, multimodality micro-imaging, such as

micro-PET/CT [12]-[13], micro-MR/PET, and micro-SPECT/CT [14]-[15], which allow fusion of functional and anatomic information, have enriched our arsenal of research tools.

A conventional laboratory micro-CT system utilizes a microfocal x-ray tube as a source of x-ray radiation. However, the microfocal x-ray tube exhibits a number of limitations, including the following: (i) limited maximum power typically does not exceed 10 W for an 8 μm focal spot [8], (ii) limited selection of the anode material (Cu, Mo, W), resulting in a very limited control of the x-ray spectrum produced, and (iii) broad x-ray spectra because, in order to achieve a very small x-ray focal spot at reasonable current (typically ~100 mA or less),

the applied cathode-anode voltage has to be high (typically above 40 keV). Emerging photonic technologies, such as ultrafast lasers, provide new opportunities for overcoming the limitations of conventional x-ray tube, allowing construction of a compact, reasonably priced, laboratory- or clinic-based x-ray source. The compactness and reasonable price distinguishes the ultrafast laser-based x-ray source (ULX) from very attractive (high brightness, flexible wavelength, etc.) but very expensive and very large synchrotron-type x-ray source that do not lend themselves to laboratory or clinical applications.

In this paper we report results of our initial exploration of ULX application to micro-CT for small animal imaging.

MATERIALS AND METHODS

The invention of chirped-pulse amplification (CPA) in the mid 1980's allowed the achievement of ultra short laser pulses and hence very high optical power density (1018-1020 W/cm²) delivered to the target by the laser beam from relatively compact (table-top) terawatt (1 TW = 10¹² W) lasers with femtosecond (1 fs = 10⁻¹⁵ s) pulse duration [16]-[17].

X-rays generation can occur when a visible or infrared laser beam is focused onto the surface of solids or liquids. When the optical power density exceeds a material dependent threshold value, usually ~10¹² W/cm², continuous bremsstrahlung and characteristic x-ray emission lines occurs from the laser-produced plasma (LPP) on the target surface [18]-[21]. The LPP x-ray focal spots created by the ultrafast lasers are very small (3-50 μm) and bright, with x-ray peak power higher than that of synchrotron sources, and many orders of magnitude higher than produced by conventional medical x-ray tubes.

Herrlin and co-workers reported the first application of an ultrafast LPP x-ray source to

radiological imaging [22]-[23]. We have demonstrated the feasibility of ultrafast lasers for mammography [24] and angiography [25]. The x-ray spectrum emitted during the interaction of the optical laser beam and the solid target is controlled by the energy distribution of the suprathreshold electrons that interact with the solid core of the target [18]-[19], [26]-[27]. The emitted hard x-ray spectrum is composed of an extended continuous bremsstrahlung emission and of discrete Ka emission lines (**Fig 1**). For low and medium Z, the Ka radiation is dominant and has been used, with appropriate filtering, in our imaging work. The continuum spectrum and the x-ray yield of the characteristic Ka emission produced by a Maxwellian electron population have been theoretically modeled and estimated [19], [27]. The x-ray spectrum produced by ultrafast laser-based x-ray source can be tailored to a specific specimen thickness and composition through selection of a suitable laser target and matching filter material. Consequently, energy-optimized x-ray spectra for imaging tasks can be generated. Elemental composition of the targets (32<Z<74) can be selected to cover the energy range of interest in micro-CT (15-60 keV) [21], [28]-[29].

RESULTS

Our measurements indicate that, when using adaptive optics, an elliptical x-ray focal spot (5 μm × 10 μm FWHM) for multiple x-ray shots can be created with the long axis parallel to the plane of incidence [29]. Without adaptive optics, the focal spot increases by factor of ~2. By using a tilted laser target (similar to mammography anode design), one can create an effective focal spot of size 5 μm × 5 μm.

The ULX source for micro-CT has a replenishable target that is renewed after each laser pulse or after a short (2-5) train of shots, so the heat load of the target resulting in target melting is not a limiting factor of the x-ray output. This is in contrast with the maximum power (around 10 W) that can be delivered by

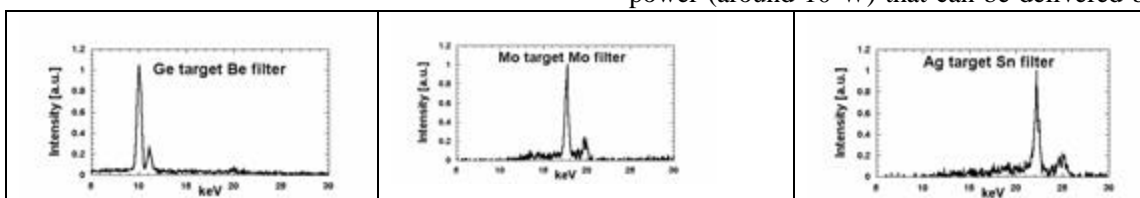


Fig. 1. The ULX x-ray spectra measured with CZT detector (Amptek) measured at the at Advanced Laser Light Source (ALLS at INRS -EMT, University of Québec)

conventional microfocal tubes [8], [30].

ULX offers multiple techniques for small animal imaging:

1. Absorption imaging:
 - a. Single energy absorption imaging
 - b. Dual energy K-edge subtraction absorption imaging
2. In-line phase-contrast imaging:
 - a. Single energy in-line phase-contrast imaging
 - b. Multiple energy in-line phase-contrast imaging

We note that conventional x-ray tube based micro-CT system allow only single energy absorption imaging.

For the soft tissue in the 15 – 35 keV energy range the phase-shift term of the complex index of refraction for x-rays is up to 1000 times higher than the absorption term that is responsible for conventional radiographic imaging. In absorption imaging the x-ray detector is relatively close to the object and the x-ray source is not spatially coherent. This is a typical situation in radiological imaging with x-ray tube. However, under certain conditions phase-shift could provide additional mechanism for image contrast formation. If the x-ray source is very highly coherent (as is in the case of ULX) and the detector is sufficiently far from the sample one can realize Fresnel “in line” geometry where image contrast is provided partially by the diffraction effects due to phase shift in the sample and partially by the absorption term. In this geometry contrast due to phase term is proportional to the Laplacian of phase-shift in the sample and it enhances images of interfaces. We performed initial evaluation of imaging performance in absorption mode and in in-line x-ray phase-contrast ULX micro-CT system. The in line tomography with ULX allows high-resolution measurements of the spatial distribution of the phase-shift and the absorption component of x-ray index of refraction in a living animal or a specimen. The examples of various types of projection images that could be used in microtomography are shown in Figs. 2 – 4.

DISCUSSION AND CONCLUSIONS

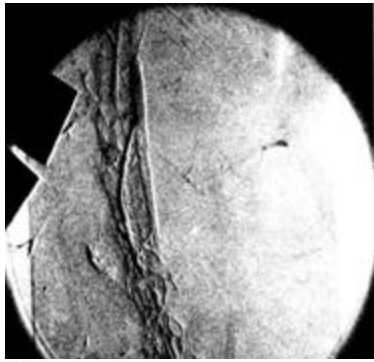
X-ray spectra produced by ultrafast laser are advantageous for micro-CT imaging, because



Fig. 2 Example of an absorption image obtained at Advanced Laser Light Source (ALLS at INRS -EMT, University of Québec). Distal hind limb and a tail of a mouse ~20 weeks old, 10 Hz laser at INRS, Mo target, Mo filter, SOD=30.0 cm, SDD=45.0 cm, intensity: 8×10^{17} W/cm², pulse duration: 70 fs, energy per pulse: 115 mJ, polarization: *p*, contrast: 10^{-10} , $\lambda=400$ nm, 4000 laser shots, hot electron temperature: 20 keV, Fuji EC-MA cassette/AD film used as an image detector.

most of the emission is in narrow characteristic lines. The spectra can be rapidly changed, via target change, and easily matched to the imaging task – e.g. animal thickness or to an absorption edge in dual-energy imaging with a contrast agent. X-ray fluence can exceed fluence produced by a conventional 10 W microfocal tube. Effective x-ray focal spot size is comparable to a microfocal tube (~ 5 μm). Good quality projection images of small animals were obtained: (a) in a single energy mode with single x-ray line matching animal thickness and density, (b) in the dual-energy mode with two x-ray lines bracketing absorption energy of the I-based and Ba-based contrast agent, respectively, and (c) in the in line phase-contrast enhancing geometry using single x-ray line matching animal thickness and density.

The ultrafast laser-based, compact, x-ray source is a promising alternative to a microfocal x-ray tube in micro-CT systems. Its utilization might result in faster scans with lower radiation dose, and with better spatial and contrast resolution. In addition, ULX might allow practical implementation of dual-energy edge subtraction



Université du Québec
Institut national de la recherche scientifique

Fig. 3 Example of a differential Gd–Nd image of a rat's vasculature containing Ba contrast agent obtained using T³ laser at INRS with Nd target and Nd filter for the low energy image and Gd target and Nd filter for the high energy image; SOD=40.0 cm, SDD= 45.0 cm, intensity: 5×10^{18} W/cm², pulse duration: 400 fs, energy per pulse: 400 mJ, polarization: *p*, contrast: 10^{10} , $\lambda=530$ nm, 200 laser shots, hot electron temperature: 25 keV, Fuji GH-1 cassette/HR-H film used as an image detector. Images were obtained at Advanced Laser Light Source (ALLS at INRS -EMT, University of Québec),

and phase-contrast micro-CT that is not possible with conventional micro-CT systems.

ACKNOWLEDGMENTS

This research has been partially sponsored by the Canadian Foundation for Innovation (CFI).

REFERENCES

1. Tai C; Chatziioannou A; Siegel S; Young J; Newport D; Goble RN; Nutt RE; Cherry SR, *Phys. Med. Biol.*, **46** (7), 1845, (2001).
2. Chatziioannou A.F.; Cherry S.R.; Shao Y.; Silverman R.W.; Meadors K.; Farquhar T.H.; Pedarsani M.; Phelps M.E., *J. Nucl. Med.*, **40** (7), 1164, (1999).
3. Cherry S. R., Y. Shao, R. W. Silverman, K. Meadors, S. Siegel, A. Chatziioannou, J. W. Young, W. Jones, J. C. Moyers, D. Newport, A. Boutefnouchet, T. H. Farquhar, M. Andreaco, M. J. Paulus, D. M. Binkley, R. Nutt, and M. E. Phelps, *IEEE Trans. on Nucl. Sci.*, **44**, (3), 1161, (1997).

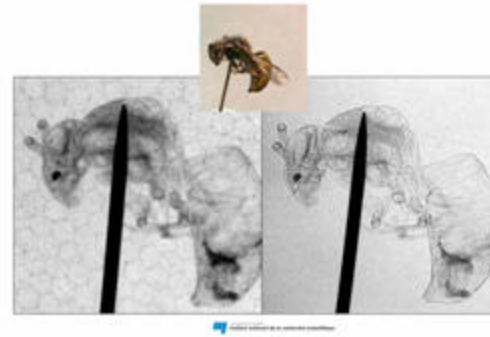


Fig. 4. *Ex vivo* raw projection images of a bee obtained with a cooled CCD camera (24 μ m pixel size, Gd₂SO₂ phosphor screen) at the Advanced Laser Light Source (ALLS at INRS -EMT, University of Québec), 10 Hz laser, Mo target, 100 μ m Mo filter; pulse duration: 50 fs, energy per pulse: 250 mJ, polarization: *p*, contrast: 10^{10} , conversion efficiency at 20 keV: 4×10^{-5} , $\lambda_{\text{laser}} = 400$ nm, hot electron temperature: 20 keV, effective x-ray focal spot $5 \times 10 \mu$ m, fluence at 20 keV: 4×10^{10} photons/(s 2π sr). Left image: source-to-object distance (SOD) = 50 cm, object-to-detector distance (ODD) = 53 cm. Right image: SOD = 50 cm, ODD = 250 cm. Exposure time 200 s. No attempt was made to extract the phase-contrast component from the image on the right. In the center the appearance of the bee in visible light is shown.

4. Kastis G. K., Barber H. B., Barrett H. H., Gifford H. C., Pang I. W., Patton D. D., Sain J. D., Stevenson G., and Wilson D. W., *J. Nucl. Med.*, **39**, (5 suppl.), 9P (1998).
5. Schramm N., A Wirtwar, F Sonnenberg, and H Halling, *IEEE Trans. on Nucl. Sci.*, **47**, (3), 1163, (2000).
6. Eccles CD and PT Callagan, *J. Magn. Reson.*, **68**, 393, (1986).
7. Turnbull DH, *Methods Mol. Biol.*, **135**, 235, (2000).
8. Paulus M. J., S. S. Gleason, S. J. Kennel, P. R. Hunsicker, and D. K. Johnson, *Neoplasia*, **2**, (1-2), 62, (2000).
9. Song X., E. C. Frey, and B. M. W. Tsui, *Conf. Rec. IEEE Nucl. Sci. Symp. and*

- Med. Imag. Conf., San Diego, CA, USA*, **3**, 1600, (2001).
10. Sasov A. and D. Dewaele, *Proc. SPIE*, **4503**, 256 (2002).
 11. Davis, G.R., F.S.L.Wong, *Physiol. Meas.*, **17**, 121, (1996)
 12. Khodaverdi M., F. Pauly, S. Weber, G. Schroder, K. Ziemons, R. Sievering, and H. Halling, *Conf. Rec. IEEE Nuc. Sci. Symp. and Med. Imag. Conf., San Diego, CA, USA*, **3**, 1605, (2001).
 13. Goertzen A. L., Meadors K., Silverman R. W., and Cherry S. R., *Mol. Imag. Biol*, **4**, (suppl. 1), S20, (2002).
 14. Iwata K., Wu M. C., and Hasegawa B. H., *Conf. Rec. IEEE Nuc. Sci. Symp. and Med. Imag. Conf., Seattle, USA*, **3**, 1608, (1999).
 15. Iwata K., MacDonald L. R., Li J., Williams S. P., Sakdinawat A. E., Hwang A. B., Wu, B. E. Patt M. C., Iwanczyk J. S., and Hasegawa B. H., *Mol. Imag. Biol.*, **4**, (suppl. 1), S21, (2002).
 16. Strickland D and Mourou G, *Opt. Commun.*, **56**, 219, (1985).
 17. Perry MD and Mourou G, *Science*, **264**, 917, (1994).
 18. Kieffer JC, Audebert P, Chaker M, Matte JP, Pepin H, Johnston, Maine P, Meyerhofer D, Delettrez J, Strickland D, Bado P and Mourou G, *Phys. Rev. Lett.*, **62**, 760 (1989).
 19. Kieffer JC, Z. Jiang, A. Ikhlef, C.Y. Cote and O. Peyrusse, *J. Opt. Soc. Am.*, **B13**, 132, (1996).
 20. Ikhlef A, Jiang Z, Kieffer JC, Krol A, *J. X-ray Sci. Techn.* **8**, 151, (1999).
 21. Yu J., Jiang Z., Kieffer J.C., and Krol A., *Physics of Plasmas*, **6**, 1318, (1999).
 22. Herrlin K, Svahn G, Olsson C, Petterson H, Tillman C, Persson A, Wahlström, and Svanberg S., *Radiology*, **189**, 65, (1993).
 23. Tillman C., Mercer I., Svanberg S. and Herrlin K., *J. Opt. Soc. Am.*, **B13**, 209, (1996).
 24. Krol A., Ikhlef, J.-C. Kieffer, D. A. Bassano, C.C. Chamberlain, Z. Jiang. H. Pepin, and S. C. Prasad, *Medical Physics*, **24**, 725, (1997).
 25. Krol, A. Jean-Claude Kieffer, Zahia Ichalale, Zhiming Jiang, Charles C. Chamberlain, and Ernest Scalzetti, *Proc. of SPIE*, **4504**, (2001).
 26. Kieffer JC, Matte JP, Pepin H, Chaker M, Beaudoin Y, Chien CY, Coe S, Mourou G, Dubau J, *Phys. Rev. Lett.*, **68**, 480, (1992).
 27. Kieffer JC, Chaker M, Cote CY, Beaudoin Y, Pepin H, Chien CY, Coe S, Mourou G., *Applied Optics*, **32**, 4247 (1993).
 28. Krol A, Kieffer JC, Jiang Z, Yu J, Chamberlain CC, Bassano DA, and Galant P, *Proceedings of SPIE*, **3659**, 734-739 (1999).
 29. Hou, B.X. J. Nees, G. Mourou, L. M. Chen, J. C. Kieffer, A. Krol, C. C. Chamberlain, *Appl. Physics Lett.*, **84**, 2259 (2004).
 30. Flynn M.J., S.M. Hames, D.A. Reiman, S.J. Wilderman, *Nuc. Instrum. Meth. Phys. Res. Sect.*, **A353**, 312, (1994)